Partially observed competing degradation processes: modeling and inference

Laurent Bordes, Sophie Mercier, Emmanuel Remy, Emilie Dautrême

Partially observed competing degradation processes: modeling and inference

Laurent Bordes[1] Sophie Mercier[1] Emmanuel Remy[2]
Emilie Dautrême[2]

[1]CNRS/Univ Pau & Pays Adour, Laboratoire de Mathématiques et de leurs Applications de Pau, Fédération IPRA, UMR5142, 64000 Pau, France
laurent.bordes@univ-pau.fr, sophie.mercier@univ-pau.fr
[2]EDF R&D – Industrial Risk Management Department, Chatou, France
emmanuel.remy@edf.fr, emilie.dautreme@edf.fr

July 12, 2016

Abstract

The aim of the present paper is the stochastic modeling and statistical inference of a component which deteriorates over time, for prediction purpose. The deterioration is due to defects which appear one by one and next independently propagate over time. The motivation comes from an application to passive components within electric power plants, where (measurable) flaw indications first initiate (one at a time) and next grow over time. The available data come from inspections at discrete times, where only the largest flaw indication is measured together with the total number of indications on each component. Though detected, too small indications cannot be measured, leading to censored observations. Taking into account this partial information coming from the field, a specific stochastic model is proposed, where the flaw indications initiate according to a Poisson process and next propagate according to competing independent gamma processes. A parametric estimation procedure is developed, tested on simulated data and then applied to the industrial case. The fitted model is next used to make some prediction over the future deterioration of each component and over its residual operating time until a specified critical degradation level is reached.

Keywords. Competing risks; Composite likelihood; Gamma process; Poisson process; Reliability theory; Residual life

1 Introduction and motivating example

1.1 Introduction

Competing risks are largely used in survival or reliability analysis when several causes of death or failure are in competition. In a reliability study, the competing risk model can be seen

as a series system, which fails whenever one of its component fails. To be more specific, let $X_1, \ldots, X_k$ be the respective lifetimes of a $k-$component system with competing risks. The lifetime of the system then is $X = \min\{X_1, \ldots, X_k\}$ and the index C such that $X = X_C$ is known as the failure cause. The failure cause is generally observed together with the system lifetime, or it may be partially observed, with $C \in \mathcal{C} \subset \{1, \ldots, k\}$. The later case is known as a masked cause of failure. In order to prevent identifiability issues that may occur when lifetimes X_j's are dependent, the lifetimes often are considered as independent. Also, the number of competing causes is generally fixed, see Crowder [8] for an overview on classical competing risks models and their application. In presence of dependency (see [21] for an example where the dependence is due to the sharing of a common frailty random variable by the competing risks), it is generally the cause specific hazard rates that are estimated. The number of competing causes may also sometimes be random, see [2] for an example in biostatistics. It seems however that the case of a random number of competing causes with non identically distributed component lifetimes has not been much addressed in the previous survival or reliability analysis literature.

In this paper, we are interested in a system subject to several competing deterioration sources (defects), which appear one at a time and next independently propagate. These defects could be for instance pits due to corrosion [13], fatigue cracks [10], or any measurable indications of deterioration which initiate over time and next propagate. In the present applicative context, these defects correspond to flaw indications, which are not further specified, due to confidentiality issues. However we use this vocabulary in the remaining of the paper, and we will speak of "flaw indication" or "indication" for short. The competing deterioration sources (the flaw indications) initiate at random times $T_1 < T_2 < \cdots$, which are the points of a counting process $\left(N_t = \sum_{i=1}^{\infty} \mathbf{1}_{\{T_i \leq t\}}\right)_{t \geq 0}$. Once initiated at time T_j, the j–th indication propagates according to a non decreasing process $Z^{(j)} = (Z_t^{(j)})_{t \geq 0}$, which is set equal to zero on $[0, T_j)$. The system is considered to be out of order as soon as the value of one among all the initiated flaw indications has reached a critical threshold, known in advance. This leads to a competition between the N_t indications present at time t. Then we call competing degradation process the bivariate process $(N_t, Z_t)_{t \geq 0}$ where $Z_t = \max\{Z_t^{(1)}, \ldots, Z_t^{(N_t)}\}$. This denomination comes from the fact that the crossing time of the degradation level ℓ by $(Z_t)_{t \geq 0}$ is nothing but the minimum of the crossing times of processes $Z^{(1)}, \ldots, Z^{(N_t)}$ for the same level. This connection between multiple degradation processes and competing risks has been used to derive new lifetime models. In [20] some examples are provided by using Brownian Maximum Processes or gamma processes for the degradation process, whereas in [11] the authors use degradation processes of type $Z_t^{(j)} = g(t; A_j)$ where g is a known function and A_i a random vector.

Though the propagation is assumed to be similar for each of the flaw indications, their initiation times are different, leading to non identically distributed $Z^{(j)}$'s and consequently, to a competition between a random number of non identical degradation processes. A similar approach has been proposed in Kuniewski et al. [13], in order to evaluate damages caused by corrosion of industrial systems in the oil industry. Their model combines a non homogeneous spatial Poisson process for the initiation process $(N_t)_{t \geq 0}$ with a homogeneous gamma process for the propagation of the defect. The parameters of both Poisson and gamma processes are assumed to be known, up to a proportionality constant for the Poisson process. The paper develops a Bayesian method for estimating the proportionality constant and predictive indicators, based on partial information data including imperfect defects detection. In [3], Caballé et al. propose a condition-based maintenance of a system subject to fatal shocks and to deterioration due to pitting corrosion, with a similar model as [13] for the latter. In the

same way, Cha and Castro envision sudden failures in competition with soft failures due to a similar deterioration model in [6], where they study some positive dependence properties between the competing failure times and some condition-based maintenance policy. A very close deterioration model is also used in [4, 25] (among others).

The paper is organized as follows. First, we introduce in the next sub-section the industrial example which motivated the study. The probabilistic model is described in Section 2, where the conditional probability density function of Z_t given N_t is calculated, together with additional prognostic indicators of interest for the application. All the calculations are relegated to Appendices A–C. In Section 3, a parametric estimation procedure is proposed, which accounts for the incomplete information data coming from the field, as described in the next sub-section. Section 4 is devoted to numerical developments, including a validation of the estimation method through a Monte Carlo study as well as the application to the real data set. Some concluding remarks are given in the last section.

1.2 Motivating industrial application

EDF, the world's biggest electricity generator, performs in-service inspections of the passive components within its electric power plants in order to ensure that their degradation is lower than a critical level and guarantee the safety and the availability of the installations. These examinations are regular but non periodic, and their times differ from one component to the other. They allow to collect successive degradation measurements for each component, from which the point is to predict the degradation propagation and estimate the residual operation time upon which the critical degradation level (denoted by ℓ) is reached.

By an examination, the measurement process does not always give a perfect image of the degradation. Indeed, because of technical limitations, too small flaw indications are detected but their size cannot be measured. Moreover, if several competing flaw indications have initiated on one component, the measurement process can count the number of existing flaw indications but only the size of the largest one can be measured. For a better understanding of the available information, let us now be more specific on the examination procedure, which is made through two non-destructive ultrasonic testing processes with different objectives and performances:

- The first process aims at detecting flaw indications: it gives a binary response "presence" or "absence" of flaw indications, together with the number of initiated indications.
- The second one is conceived to measure flaw indications. The measurement first requires the detection of an indication by this second process, which is less sensitive than the first one and only detects flaw indications whose measurement exceeds a known fixed threshold. Also, due to the use of two different technologies for this second process, there are several (always known) thresholds under which the flaw indication cannot be measured. Finally, when several flaw indications are observable, only the largest one is measured by the second testing process.

We assume that all flaw indications are detected by the first testing process and that the second testing process gives the exact measurement of the largest indication when observable. The available data concern 228 components that are supposed to be independent and identical. The commissioning date is known for each component as well as its inspection times. Each

previously described two-step examination provides one of the possible following information about the degradation level:

- No flaw indication is detected on the component: no indication is initiated at the inspection time.
- At least one flaw indication is detected by the first testing process at the inspection time but no flaw indication is detected by the second testing process: the number of initiated indications is known and the measurement of the largest flaw is lower than a deterministic known value (left censoring).
- The second testing process detects and measures flaw indications: the number of initiated indications is known, as well as the measurement of the largest indication on the component (which is therefore higher than a known value).

In order to make accurate degradation predictions, it is essential to take into account this partial information coming from the field. It is important to mention that no other source of information is available to predict the evolution of the indications with time. In particular, the underlying physical phenomena are complex and no representative mechanical model exists: a structural reliability approach [14] is thus not feasible. The measurements from the inspections are the only available material and a statistical analysis of these data is the unique way to assess the residual lifetime of the components.

The object of the present study is to compute predictive indicators such as the yearly expected number of initiated flaw indications, the expected annual growth of one flaw indication, quantiles of the residual operating time given some observations at a given time. Another applicative object is the study of the influence of the number of initiated flaw indications on the residual operating time, in order to know whether it is worth or not to gather this information from the field. A last point of interest from an industrial point of view is to know whether it is worth taking into account censoring. To be more specific, a first possibility for estimating the model parameters naturally is to take into account the censoring nature of the data. A second possibility is to use the so-called imputation method deployed within survival analysis studies. In this method, the censoring level of any censored data is considered to be the data itself. Here, considering a largest flaw indication which is known to be smaller than a censoring level C, the imputation method consists in considering that the size of the largest flaw indication is exactly equal to C. (And this is done for all the censored data). Of course, this imputation method leads to an over-estimation of the real sizes of the (largest) flaw indications and hence introduces some bias in the estimated parameters. However, it may be of interest in an industrial context because it leads to simpler estimation procedures. More important, the method has the good property of being conservative, in the sense that the results over-estimate the degradation propagation and hence provide pessimistic prognostic indicators. (Such a method is particularly adapted as soon as safety is concerned). The point here is to know whether the imputation method provides very different results from an estimation procedure taking into account the censoring nature of the data and hence whether it is worth taking into account censoring. The answer to this question requires the development of the two different estimation procedures, for comparison purpose.

2 Competing degradation model and prognostic indicators

2.1 Competing stochastic degradation processes

We here specify the stochastic model for the initiation and development of flaw indications on one single component. We first set N_t to be the random number of indications already initiated at time t. The points of the counting process $(N_t)_{t\geq 0}$ stand for the initiating times of the flaw indications on the component and are denoted by $T_1, T_2, \ldots$, with $0 < T_1 < T_2 < \cdots$ (almost surely). In case $N_t \geq 1$, we set $Z_t^{(j)}$ to be the (random) measurement of the j-th flaw indication at time t, with $1 \leq j \leq N_t$. The measurement of the largest flaw indication at time t hence is:

$$Z_t = \begin{cases} \max\limits_{1\leq j\leq N_t} \left(Z_t^{(j)}\right) \text{ if } N_t \geq 1, \\ 0 \text{ elsewhere.} \end{cases}$$

If $0 \leq t_1 < \cdots < t_m$ are the inspection times of the component (different from one component to another and non informative), data for one component are $(n_j, z_j)_{1\leq j\leq m}$ with $n_j = N_{t_j}(\omega)$ and $z_j = Z_{t_j}(\omega)$ for an experiment ω. These data correspond to partial observation $\left(N_{t_j}, Z_{t_j}\right)_{1\leq j\leq m}$ of the competing degradation process $(N_t, Z_t)_{t\geq 0}$.

In order to account several possible levels of censoring at time t, we set C_t to be the known deterministic censoring level at time t. We also introduce a censoring indicator:

$$D_t = \begin{cases} 0 \text{ if } Z_t \leq C_t, \\ 1 \text{ otherwise.} \end{cases}$$

The data now are of the form $(n_j, u_j, d_j)_{1\leq j\leq m}$ with $n_j = N_{t_j}(\omega)$, $u_j = U_{t_j}(\omega)$, $d_j = D_{t_j}(\omega)$, and correspond to one observation of $\left(N_{t_j}, U_{t_j}, D_{t_j}\right)_{1\leq j\leq m}$ with

$$U_t = \begin{cases} Z_t & \text{if } Z_t > C_t, \\ C_t & \text{if } Z_t \leq C_t \text{ and } N_t > 0, \\ 0 & \text{otherwise.} \end{cases}$$

An example of censored trajectory is provided in Figure 1 for the competing degradation process. The censoring level is assumed to be constant for sake of clarity. Four flaw indications initiate at time T_1 (blue), T_2 (red), T_3 (green) and T_4 (black), respectively. At the beginning, the largest indication (namely Z_t) is the blue one, next the red one and finally the green one. This is depicted through black/white dots, where black dots means that Z_t is below the censoring level (so that $U_t = C_t$) and white dots refers to an observable Z_t beyond the censoring level (so that $U_t = Z_t$). The observable counting process $(N_t)_{t\geq 0}$ is simultaneously increased by one at each initiation time $T_i, i = 1, \ldots, 4$.

Assumptions. We assume that the degradation processes are identical for all the components and that they are independent between components. The independence is justified by the fact that the components are in different production units throughout France so that they do not interfere one with the other. We also assume that once initiated, the processes defining the propagation of all flaw indications present on one component are independent and identically distributed (i.i.d.). Indeed there are only few flaw indications at the same time on a component (otherwise the component is changed) and the size of a component is "large" (thus limiting some

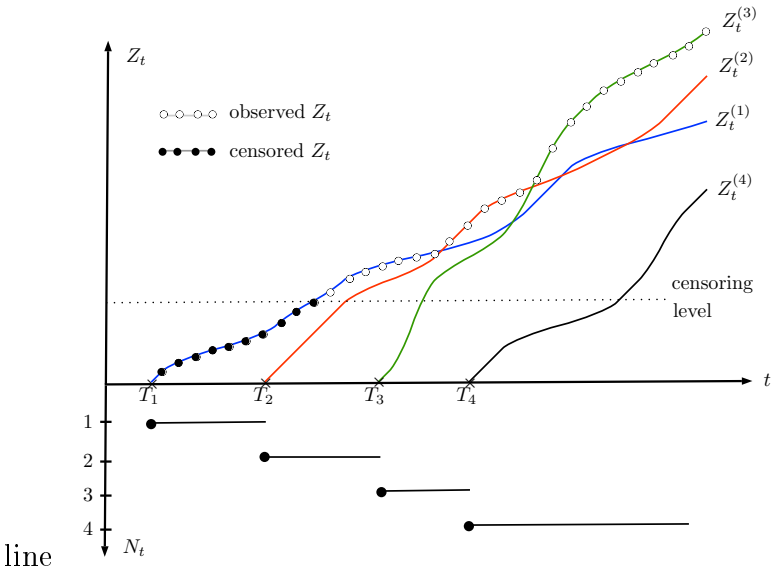

line

Figure 1: An example of trajectory for the competing degradation process

potential mechanical interactions between flaw indications), so that it seems mostly natural to assume that the development of the different flaw indications are similar and independent one from the other. Note that this i.i.d. assumption is pretty classical when dealing with similar problems, see for instance [3], [4], [5], [13], [19] or [25] among lots of others. For each component, the number of flaw indications is assumed to follow a Poisson process $(N_t)_{t\geq 0}$, where N_t is Poisson distributed with parameter $\Lambda(t)$ and distribution denoted by $\mathcal{P}(\Lambda(t))$, see [18] for more details on Poisson processes. In the sequel, we either suppose that this process is homogeneous (HP) with $\Lambda(t) = \lambda t$, or non homogeneous (NHP) with $\Lambda(t) = \alpha t^{\beta}$ (power-law process), where $\lambda, \alpha, \beta > 0$. The rate of this Poisson process is denoted by $\lambda(t)$, with $\lambda(t) = \lambda$ for the HP process and $\lambda(t) = \Lambda'(t) = \alpha\beta t^{\beta-1}$ for the NHP process. When a flaw indication appears, we assume that its measurement increases according to a gamma process with parameters $(A(t), b)$, e.g. see [1, 12, 22, 26] for more details on the use of gamma processes for modeling deterioration. Here again, we envision the homogeneous case (HG) with $A(t) = at$ and the non homogeneous case (NHG) with $A(t) = \eta t^{\gamma}$, where $a, \eta, \gamma > 0$.

To specifically define the measurements of the various indications present on a component at time t, we introduce a sequence $\left(X^{(j)}\right)_{j\in\mathbb{N}^*}$ of independent gamma processes, all with parameters $(A(t), b)$. For each $j \in \mathbb{N}^*$ and each $t \geq 0$, the random variable $X_t^{(j)}$ is gamma distributed with probability density function (p.d.f.) $f_{A(t),b}(x) = b^{A(t)}x^{A(t)-1}e^{-bx}\mathbf{1}_{\mathbb{R}_+}(x)/\gamma(A(t))$, cumulative distribution function (c.d.f.) denoted by $F_{A(t),b}$ and survival function denoted by $\bar{F}_{A(t),b}$ where $\bar{F}_{A(t),b} = 1 - F_{A(t),b}$. With the previous notations, we have $\mathbb{E}\left(X_t^{(j)}\right) = A(t)/b$ and $\mathrm{var}\left(X_t^{(j)}\right) = A(t)/b^2$.

For each $1 \leq j \leq N_t$, the difference $t - T_j$ corresponds to the elapsed time at time t since the initiation of the j-th indication. We then set $Z_t^{(j)} = X_{t-T_j}^{(j)}$ to be the measurement of the j-th flaw indication at time t. If $j > N_t$, the j-th indication has not yet been initiated at time t and we put $Z_t^{(j)} = 0$. Setting $(t - T_j)^+ = \max(t - T_j, 0)$ and remembering that $X_0^{(j)} = 0$, this

can be summed up into

$$Z_t^{(j)} = X^{(j)}_{(t-T_j)^+} \text{ for all } j \in \mathbb{N}^*.$$

As only the largest flaw indication can be measured by an examination, without censoring, a measure at time t hence is an observation of

$$Z_t = \max_{j\in\mathbb{N}^*}\left(Z_t^{(j)}\right) = \begin{cases} \max\limits_{1\leq j\leq N_t}\left(X^{(j)}_{t-T_j}\right) & \text{if } N_t \geq 1, \\ 0 \text{ otherwise.} \end{cases}$$

We now derive some probabilistic results, to be used later on for inference purpose and computation of the predictive indicators.

2.2 Probabilistic results

Let us first remark that the maximum among the $Z_t^{(j)}$'s will generally not correspond to the same trajectory over time. A direct consequence is that the distribution of an increment $Z_t - Z_{t_0}$ (with $t_0 < t$) is not an easy thing to write down. Also, the process $(Z_t)_{t\geq 0}$ does not have independent increments. The obtaining of probabilistic results hence requires some care, especially for the derivation of the conditional distribution of (Z_t, N_t) given (Z_{t_0}, N_{t_0}) given in Proposition 2.

We first provide the conditional distribution of Z_t when the number of flaw indications is known at time t.

Proposition 1 *Given that $N_t = 0$, then Z_t is conditionally almost surely null (namely $\mathbb{P}(Z_t = 0|N_t = 0) = 1$). Otherwise, for each $n \geq 1$, the conditional distribution of Z_t given that $N_t = n$ has the following cumulative distribution function (c.d.f.)*

$$F_{Z_t|N_t}(z|n) = \left\{\frac{\int_0^t F_{A(y),b}(z)\,\lambda(t-y)\,dy}{\Lambda(t)}\right\}^n, \tag{1}$$

and its probability distribution function (p.d.f.) with respect to the Lebesgue measure is given by

$$f_{Z_t|N_t}(z|n) = \frac{n}{(\Lambda(t))^n}\left\{\int_0^t f_{A(y),b}(z)\,\lambda(t-y)\,dy\right\}\left\{\int_0^t F_{A(y),b}(z)\,\lambda(t-y)\,dy\right\}^{n-1} \tag{2}$$

for all $z \geq 0$.

Proof. See Appendix A. □

The joint distribution of (Z_t, N_t) is easy to derive as the product of the conditional distribution of Z_t given N_t cross the distribution of N_t (see also Equation (B.3) in Appendix B). It admits the following density function

$$f_{(N_t,Z_t)}(n,z) = \begin{cases} e^{-\Lambda(t)} & \text{if } n = 0, \\ \frac{e^{-\Lambda(t)}}{(n-1)!}\left\{\int_0^t f_{A(y),b}(z)\,\lambda(t-y)\,dy\right\}\left\{\int_0^t F_{A(y),b}(z)\,\lambda(t-y)\,dy\right\}^{n-1} & \text{if } n > 0 \end{cases} \tag{3}$$

with respect to

$$\delta_0(dn) \times \delta_0(dz) + \sum_{k=1}^{+\infty} \delta_k(dn) \times dz.$$

We now provide conditional distribution results of the competing degradation process at a time $t > 0$ given its value at a previous time $t_0 \in [0, t)$.

Proposition 2 *For $t_0 \in [0, t)$ and $z \geq 0$ we have*

$$\mathbb{P}(Z_t \leq z | Z_{t_0} = 0) = e^{-(\Lambda(t)-\Lambda(t_0))+\int_{t_0}^{t} F_{A(t-v),b}(z)\lambda(v)dv} = e^{-\int_{t_0}^{t} \bar{F}_{A(t-v),b}(z)\lambda(v)dv}. \tag{4}$$

For $t_0 \in (0, t)$, $0 < z_0 \leq z$ and $n \geq n_0 \geq 1$, we have

$$\begin{aligned}
&\mathbb{P}(Z_t \leq z, N_t = n | Z_{t_0} = z_0, N_{t_0} = n_0) \\
&= e^{-(\Lambda(t)-\Lambda(t_0))} \times \frac{\int_0^{t_0} F_{A(t-u)-A(t_0-u),b}(z - z_0) f_{A(t_0-u),b}(z_0) \lambda(u) du}{\int_0^{t_0} f_{A(t_0-y),b}(z_0) \lambda(y) dy} \\
&\times \left(\frac{\int_0^{t_0} \left(\int_0^{z_0} F_{A(t-u)-A(t_0-u),b}(z - x) f_{A(t_0-u),b}(x) dx \right) \lambda(u) du}{\int_0^{t_0} F_{A(t_0-y),b}(z_0) \lambda(y) dy} \right)^{n_0-1} \\
&\times \frac{\left(\int_{t_0}^{t} F_{A(t-v),b(z)} \lambda(v) dv \right)^{n-n_0}}{(n - n_0)!}.
\end{aligned} \tag{5}$$

Proof. See Appendix B. □

Note that a similar expression to (4) is provided by Equation (18) in [13] in the specific case of a homogeneous gamma process with $t_0 = 0$.

Writing

$$\mathbb{P}(Z_t \leq z | Z_{t_0} = z_0, N_{t_0} = n_0) = \sum_{n=n_0}^{+\infty} \mathbb{P}(Z_t \leq z, N_t = n | Z_{t_0} = z_0, N_{t_0} = n_0),$$

one immediately gets the following corollary.

Corollary 1 *For $0 < t_0 < t$, $0 < z_0 \leq z$ and $n_0 \geq 1$, we have*

$$\begin{aligned}
&\mathbb{P}(Z_t \leq z | Z_{t_0} = z_0, N_{t_0} = n_0) \\
&= e^{-\int_{t_0}^{t} \bar{F}_{A(t-v),b}(z)} \lambda(v) dv \times \frac{\int_0^{t_0} F_{A(t-u)-A(t_0-u),b}(z - z_0) f_{A(t_0-u),b}(z_0) \lambda(u) du}{\int_0^{t_0} f_{A(t_0-y),b}(z_0) \lambda(y) dy} \\
&\times \left(\frac{\int_0^{t_0} \left(\int_0^{z_0} F_{A(t-u)-A(t_0-u),b}(z - x) f_{A(t_0-u),b}(x) dx \right) \lambda(u) du}{\int_0^{t_0} F_{A(t_0-y),b}(z_0) \lambda(y) dy} \right)^{n_0-1}.
\end{aligned}$$

If necessary, one could also derive from the previous results the conditional distribution of Z_t given Z_{t_0} (and next the distribution of an increment $Z_t - Z_{t_0}$) by writing

$$\mathbb{P}\left(Z_t \leq z | Z_{t_0} = z_0\right) = \sum_{n_0=1}^{\infty} \mathbb{P}(Z_t \leq z | Z_{t_0} = z_0, N_{t_0} = n_0) \frac{\mathbb{P}(Z_{t_0} = z_0, N_{t_0} = n_0)}{\mathbb{P}(Z_{t_0} = z_0)}$$

for all $z_0 > 0$ and using the joint distribution of (Z_{t_0}, N_{t_0}) provided by Equation (B.3) in Appendix B. This is not used in the following and consequently not made explicit here.

2.3 Prognostic indicators

The initiation time U of the first flaw indication verifies $\mathbb{P}(U > t) = \mathbb{P}(N(t) = 0) = e^{-\Lambda(t)} = e^{-\alpha t^{\beta}}$. It is therefore distributed according to a Weibull distribution with scale parameter $\alpha^{-1/\beta}$ and shape parameter β. Mean, variance and quantiles of the distribution of U are given in Table 1.

Table 1: Main characteristics of the initiation time of the first flaw indication

Mean	Variance	Quantile of order ε
$\mu_c = \alpha^{-1/\beta}\gamma\left(1 + 1/\beta\right)$	${\sigma_c}^2 = \alpha^{-2/\beta}\gamma\left(1 + 2/\beta\right) - {\mu_c}^2$	$q_{c,\varepsilon} = \alpha^{-1/\beta}\left(-\log\left(1 - \varepsilon\right)\right)^{1/\beta}$

In our model, the propagation of a flaw indication follows a gamma process with parameters $(A(t), b)$ and the expected propagation between times s and t (for $0 < s < t < \infty$) is $(A(t) - A(s))/b$. For a homogeneous gamma process with parameters (a, b), the yearly expected propagation is $365\, a/b$ since the time unit is the day.

Remembering that ℓ stands for the critical degradation level of the system, we set τ_ℓ to be the crossing time of level ℓ, with

$$\tau_\ell = \inf\{t \geq 0 : Z_t > \ell\}.$$

Given $t_0 \geq 0$ and an observation $(Z_{t_0}, N_{t_0}) = (z_0, n_0)$ at time t_0 with $z_0 \in [0, \ell)$ (so that $\tau_\ell > t_0$), the residual life of a component at time t_0 is identically distributed as the conditional distribution of $\tau_\ell - t_0$ given $(Z_{t_0}, N_{t_0}) = (z_0, n_0)$. Given ε in $(0, 1)$, a prognostic indicator of major interest for the industrial application is the quantile $t_\varepsilon^{(\ell, t_0, z_0, n_0)}$ of order ε of the residual life at time t_0 given that $Z_{t_0} = z_0$ and $N_{t_0} = n_0$. For $z_0 = 0$, we necessarily have $n_0 = 0$ so that we write $t_\varepsilon^{(\ell, t_0, 0)}$ instead of $t_\varepsilon^{(\ell, t_0, 0, 0)}$.
The quantile $t_\varepsilon^{(\ell, t_0, z_0, n_0)}$ verifies

$$\mathbb{P}\left(\tau_\ell - t_0 < t_\varepsilon^{(\ell, t_0, z_0, n_0)} | Z_{t_0} = z_0, N_{t_0} = n_0\right) = \varepsilon,$$

or equivalently

$$\mathbb{P}\left(Z_{t_\varepsilon^{(\ell, t_0, z_0, n_0)} + t_0} \leq \ell | Z_{t_0} = z_0, N_{t_0} = n_0\right) = 1 - \varepsilon,$$

using the fact that $\{\tau_\ell \geq t\} = \{Z_t \leq \ell\}$. Based on Equation (4) or Corollary 1 according to whether $z_0 = 0$ or $z_0 > 0$, respectively, it is now easy to write down the equation fulfilled by the quantile $t_\varepsilon^{(\ell, t_0, z_0, n_0)}$. As will be seen later on, the model that we finally retain for the application is the combination of the NHP process with the HG process (denoted by NHP–HG model) so that the equation fulfilled by the quantile $t_\varepsilon^{(\ell, t_0, z_0, n_0)}$ is given only under this assumption.

Proposition 3 *Assume that $(N_t, Z_t)_{t\geq 0}$ follows the NHP–HG model. For $z_0 = 0$ the quantile $t_\varepsilon^{(\ell,t_0,0)}$ is obtained by solving*

$$\int_0^{t_\varepsilon^{(\ell,t_0,0)}} \bar{F}_{ay,b}(\ell) \left(t_\varepsilon^{(t_0,0)} + t_0 - y\right)^{\beta-1} dy = -\frac{\log(1-\varepsilon)}{\alpha\beta}. \tag{6}$$

For $z_0 \in (0,\ell)$ the quantile $t_\varepsilon^{(\ell,t_0,z_0,n_0)}$ is obtained by solving

$$\begin{aligned}
&\log\left\{F_{a\, t_\varepsilon^{(\ell,t_0,z_0,n_0)},b}(\ell - z_0)\right\} - \alpha\beta \int_0^{t_\varepsilon^{(\ell,t_0,z_0,n_0)}} (u+t_0)^{\beta-1} \bar{F}_{a\left(t_\varepsilon^{(\ell,t_0,z_0,n_0)}-u\right),b}(\ell)\, du \\
&+ (n_0-1) \times \log\left\{\int_0^{t_0} u^{\beta-1} \left(\int_0^{z_0} F_{a\, t_\varepsilon^{(\ell,t_0,z_0,n_0)},b}(\ell - x)\, f_{a(t_0-u),b}(x)\, dx\right) du\right\} \\
&= \log(1-\varepsilon) + (n_0-1)\log\left\{\int_0^{t_0} F_{a(t_0-y),b}(z_0)\, y^{\beta-1} dy\right\}.
\end{aligned} \tag{7}$$

Proof. See Appendix C. □

3 Estimation procedure

3.1 Estimation principle

Remember that our data are independent observations of random vectors $\left(N_{t_j}, Z_{t_j}\right)_{1\leq j\leq m}$, possibly censored, where the number of inspections m and the inspection times t_j are different from one component to another. As the increments of $(N_t, Z_t)_{t\geq 0}$ are not independent, it is a real challenge to obtain the joint distribution of $\left(N_{t_j}, Z_{t_j}\right)_{1\leq j\leq m}$. It is however possible to write down a recursive formula, which unfortunately is of no real help for the computation of the joint distribution, due to its complexity. The usual maximum likelihood method cannot hence be used. Using the joint density function of (N_{t_j}, Z_{t_j}) provided by (3), it is possible to write down a composite likelihood function (whose formal definition has been introduced by Lindsay [15]) based on the product of the likelihood of each observation with

$$\mathcal{L}\left(\theta \middle| (n_j, z_j)_{1\leq j\leq m}\right) = \prod_{1\leq j\leq m} f_{(N_{t_j},Z_{t_j})}(n_j, z_j; \theta),$$

where θ stands for the set of parameters to be estimated. In that case, the optimization is made with respect to all parameters in one single step (with five parameters for the NHP-NHG model for instance). This method has been tested on simulated data. However, the results were not very stable and the following two-step procedure has been preferred for its numerical robustness.

Let us recall that the parameters to be estimated are:

- Parameter(s) of the Poisson process: $\theta_P = \lambda$ (HP) or $\theta_P = (\alpha, \beta)$ (NHP),
- Parameters of the gamma process: $\theta_G = (a, b)$ (HG) or $\theta_G = (\eta, \gamma, b)$ (NHG).

As a first step, we classically estimate the parameter θ_P of the Poisson process by the usual maximum likelihood method, based on the uncensored observation of $\left(N_{t_j}\right)_{1\leq j\leq m}$and on the joint distribution of $\left(N_{t_j}\right)_{1\leq j\leq m}$. The estimator is denoted by $\hat{\theta}_P$.

As a second step, the parameters of the gamma processes are next estimated, plugging the estimator of the Poisson parameter into some composite likelihood function (see [7] and [23]), based on the conditional distribution of the Z_{t_j}'s given N_{t_j}'s. More specifically, we consider the following composite likelihood:

$$\mathcal{L}\left(\theta_G|\left(z_j\right)_{1\leq j\leq m},\left(n_j\right)_{1\leq j\leq m};\hat{\theta}_P\right)=\prod_{\substack{1\leq j\leq m\\ \text{s.t. } n_j\geq 1}} f_{Z_{t_j}|N_{t_j}}\left(z_j|n_j;\theta_G,\hat{\theta}_P\right),$$

where $f_{Z_{t_j}|N_{t_j}}\left(z_j|n_j;\theta_G,\hat{\theta}_P\right)$ is the conditional p.d.f. of Z_{t_j} given that $N_{t_j}=n_j$ with respect to Lebesgue measure for $n_j\geq 1$ (see Proposition 1), and where θ_P is replaced by $\hat{\theta}_P$.

Observations for which $n_j=0$ do not contain any information on θ_G because $N_{t_j}=0$ implies that $Z_{t_j}=0$. That is why only data such that $n_j\geq 1$ are involved in the likelihood function.

In practice, N independent components are observed. Adding exponent (i) to both processes and observations related to the i-th component, the log-composite-likelihood can be written as

$$\ell\left(\theta_G|\mathbf{z},\mathbf{n},\mathbf{t};\hat{\theta}_P\right)=\sum_{i=1}^{N}\sum_{\substack{1\leq j\leq m^{(i)}\\ \text{s.t. } n_j^{(i)}\geq 1}}\log\left\{f_{Z_{t_j^{(i)}}|N_{t_j^{(i)}}}\left(z_j^{(i)}|n_j^{(i)};\theta_G,\hat{\theta}_P\right)\right\}$$

where $\mathbf{z}=\left(z_j^{(i)}\right)_{\substack{1\leq j\leq m^{(i)}\\ 1\leq i\leq N}}$, $\mathbf{n}=\left(n_j^{(i)}\right)_{\substack{1\leq j\leq m^{(i)}\\ 1\leq i\leq N}}$ and $\mathbf{t}=\left(t_j^{(i)}\right)_{\substack{1\leq j\leq m^{(i)}\\ 1\leq i\leq N}}$.

If in addition we take into account censoring, we get:

$$\begin{aligned}&\ell\left(\theta_G|\mathbf{u},\mathbf{n},\mathbf{t},\mathbf{d};\hat{\theta}_P\right) \qquad (8)\\ &=\sum_{i=1}^{N}\sum_{\substack{1\leq j\leq m^{(i)}\\ \text{s.t. } n_j^{(i)}\geq 1}} d_j^{(i)}\log\left\{f_{Z_{t_j^{(i)}}|N_{t_j^{(i)}}}\left(u_j^{(i)}|n_j^{(i)};\theta_G,\hat{\theta}_P\right)\right\}+\left(1-d_j^{(i)}\right)\log\left\{F_{Z_{t_j^{(i)}}|N_{t_j^{(i)}}}\left(u_j^{(i)}|n_j^{(i)};\theta_G,\hat{\theta}_P\right)\right\}\end{aligned}$$

with $u_j^{(i)}=z_j^{(i)}$ if $d_j^{(i)}=1$ and $u_j^{(i)}=c_j^{(i)}$ otherwise, and $\mathbf{d}=\left(d_j^{(i)}\right)_{\substack{1\leq j\leq m^{(i)}\\ 1\leq i\leq N}}$.

3.2 Fitting the Poisson process

Parameter θ_P of the Poisson process can be estimated from data $(\mathbf{n},\mathbf{t})$ by maximizing the log-likelihood function:

$$\ell\left(\theta_P|\mathbf{t},\mathbf{n}\right)=\sum_{i=1}^{N}\log\left[\mathbb{P}\left(\cap_{j=1}^{m^{(i)}}\left\{N_{t_j^{(i)}}=n_j^{(i)}\right\}\right)\right].$$

Using the independent increments of $(N_t)_{t\geq 0}$, we easily get:

$$\log\left[\mathbb{P}\left(\cap_{j=1}^{m}\left\{N_{t_j}=n_j\right\}\right)\right] \propto -\Lambda\left(t_m\right)+\sum_{j=0}^{m-1}\left(n_{j+1}-n_j\right)\log\left(\Lambda\left(t_{j+1}\right)-\Lambda\left(t_j\right)\right)$$

for all $0=t_0<t_1<\cdots<t_m$ and $0=n_0\leq n_1\leq\cdots\leq n_m$, where $\propto$ means "is equal to" up to an additive constant independent of the parameter of interest (here θ_P).

The log-likelihood can then be written as

$$\ell\left(\theta_P|\mathbf{t},\mathbf{n}\right) \propto -\sum_{i=1}^{N}\Lambda\left(t_{m^{(i)}}^{(i)}\right)+\sum_{i=1}^{N}\sum_{j=0}^{m^{(i)}-1}\left(n_{j+1}^{(i)}-n_j^{(i)}\right)\log\left(\Lambda\left(t_{j+1}^{(i)}\right)-\Lambda\left(t_j^{(i)}\right)\right),$$

where we set $t_0^{(i)}=n_0^{(i)}=0$, for all $1\leq i\leq N$.

In case of a non homogeneous Poisson process, we have $\Lambda\left(t\right)=\alpha t^{\beta}$ and $\theta_P=(\alpha,\beta)$. Fixing β and solving $\frac{\partial\mathcal{L}}{\partial\alpha}\left(\alpha,\beta|\mathbf{t},\mathbf{n}\right)=0$ leads to

$$\alpha(\beta)=\frac{\sum_{i=1}^{N}n_{m^{(i)}}^{(i)}}{\sum_{i=1}^{N}\left(t_m^{(i)}\right)^{\beta}}. \tag{9}$$

We replace α by $\alpha(\beta)$ in the log-likelihood function, and then we look for the maximizer $\hat{\beta}$ of

$$\begin{aligned}&\ell\left(\beta|\mathbf{t},\mathbf{n}\right)\equiv\ell\left(\alpha(\beta),\beta|\mathbf{t},\mathbf{n}\right) \qquad (10)\\ &\propto -\left(\sum_{i=1}^{N}n_{m^{(i)}}^{(i)}\right)\log\left(\sum_{i=1}^{N}\left(t_{m^{(i)}}^{(i)}\right)^{\beta}\right)+\sum_{i=1}^{N}\sum_{j=0}^{m^{(i)}-1}\left(n_{j+1}^{(i)}-n_j^{(i)}\right)\log\left(\left(t_{j+1}^{(i)}\right)^{\beta}-\left(t_j^{(i)}\right)^{\beta}\right).\end{aligned}$$

Using a numerical optimization method, we first obtain $\hat{\beta}$; then we set $\hat{\alpha}=\alpha(\hat{\beta})$.

3.3 Fitting the gamma process

The parameter θ_G of the gamma process is estimated from $(\mathbf{u},\mathbf{n},\mathbf{t},\mathbf{d})$ by maximizing the log-composite-likelihood function given by (8). Setting $\hat{\lambda}(t)=\lambda(t;\hat{\theta}_P)$ and plugging formulae (1) and (2) into (8), we obtain

$$\begin{aligned}\ell\left(\theta_G|\mathbf{u},\mathbf{n},\mathbf{t},\mathbf{d};\hat{\theta}_P\right) \propto \sum_{i=1}^{N}\sum_{\substack{1\leq j\leq m^{(i)}\\ \text{s.t. } n_j^{(i)}\geq 1}}&\left[d_j^{(i)}\log\left(\int_0^{t_j^{(i)}}f_{A(y),b}\left(u_j^{(i)}\right)\hat{\lambda}\left(t_j^{(i)}-y\right)dy\right)\right.\\ &\left.+\left(n_j^{(i)}-d_j^{(i)}\right)\log\left(\int_0^{t_j^{(i)}}F_{A(y),b}\left(u_j^{(i)}\right)\hat{\lambda}\left(t_j^{(i)}-y\right)dy\right)\right]. \qquad (11)\end{aligned}$$

In case of a homogeneous gamma process, $A(y)$ is replaced by ay in (11). Parameters (a,b) are estimated by $(\hat{a},\hat{b})$ which maximize $\ell\left(a,b|\mathbf{u},\mathbf{n},\mathbf{t},\mathbf{d};\hat{\theta}_P\right)$. In case of a non homogeneous gamma process, $A(y)$ is replaced by ηy^{γ} in (11). Parameters (η,γ,b) are estimated by $\left(\hat{\eta},\hat{\gamma},\hat{b}\right)$ which maximizes $\ell\left(\eta,\gamma,b|\mathbf{u},\mathbf{n},\mathbf{t},\mathbf{d};\hat{\theta}_P\right)$.

3.4 Estimating the prognostic indicators

Prognostic indicators of Section 2.3 are estimated by substituting the unknown parameters of both the initiation and degradation process by their estimated values. For instance, the estimator $\hat{t}_\varepsilon^{(\ell,t_0,z_0,n_0)}$ (resp. $\hat{t}_\varepsilon^{(\ell,t_0,0)}$) of $t_\varepsilon^{(\ell,t_0,z_0,n_0)}$ (resp. $t_\varepsilon^{(\ell,t_0,0)}$) is obtained by solving (7) (resp. (6)) replacing parameters (a,b,α,β) by $(\hat{a},\hat{b},\hat{\alpha},\hat{\beta})$.

4 Numerical study

4.1 Monte Carlo simulations

This section is devoted to a simulation study which beyond checking the validity of our estimation method aims at quantifying the influence of the censoring process on the estimators behaviour. The next section deals with the application to the EDF data. As already mentioned, EDF data are well fitted by combining the NHP process with the HG process. That is why the present section is limited to this specific NHP–HG model although the estimation method has also been validated by a similar Monte Carlo study for the three other models.

In the EDF data, we have at our disposal 228 time data sets, which each corresponds to the sequence of observation times for one component. In all the simulation study, the observation times of one component are chosen among these 228 time data sets up to a fixed multiplicative constant. This rescaling of the time data through a multiplicative constant allows us to prevent from numerical instability and overflow. The same rescaling is used for the application to EDF data in the next sub-section. Several possibilities are considered for the number N of observed components, with the following choice of time data sets: for $N = 228$, we simply take all the available 228 (rescaled) time data sets; for $N = 4 \times 228 = 912$, each of the 228 time data sets is used four times; for $N = 25$, 50 and 100, the N time data sets are chosen randomly among the 228 available data sets, by sampling without replacement. Once the observation times are given for each component, the degradation samples are generated according to the NHP–HG model. In order to be as close as possible from the EDF data, the simulated data are next censored with a fixed censoring level c (which means that any indication measurement with size below c is left censored by c). In each of the following examples, the censoring level c is chosen such that the proportion of censored data is around 9%, which is similar to the EDF data. This procedure provides us with a simulated censored data set based on the observation of N components, which is next used to derive an estimation of each parameter. This procedure is independently repeated 500 times, and confidence intervals (CI) are finally constructed from empirical quantiles based on these 500 estimations. All the computations of this section have been carried out with `MATLAB` [16] on a dual core laptop computer. The optimization is made with the function `fmincon` through an interior-point algorithm and the BFGS method (please see `MATLAB` documentation on the `fmincon` function for more details and references).

As announced in the introduction, two different estimation methods are tested, first through the imputation method (namely considering censoring levels as observed measurements) and next taking into account the censoring.

A first set of parameters is considered for both methods: parameters of the NHP process with cumulative intensity $\Lambda(t) = \alpha t^\beta$ are equal to $(\alpha,\beta) = (1, 1.5)$. Parameters of the HG process are equal to $(a,b) = (1,2)$. The censoring level is $c = 0.2$.

Estimation without taking into account censoring (imputation method). We use the log-composite-likelihood function (11) with all $d_j^{(i)}$'s equal to 1. Results are provided in Table 2. As for the parameters (α, β) of the NHP process, we observe that they are well estimated, both from a bias and standard deviation point of view. Whatever the sample size is, the confidence intervals always contain the true values of the parameters. This good behaviour is consistent with the fact that the imputation method does not affect the number of indications at observation times and consequently does not affect the estimation procedure of the Poisson process parameters.
The results concerning the HG process are not convincing. Indeed, even if empirical means are not too far from their true values, we can see that there is some bias on the estimates of parameters a and b. As a matter of fact, confidence intervals are either very large (for small N) or do not even contain the true values of the parameters (for large N). Though the bias can be seen to be less important on the mean rates per unit time of both mean (a/b) and variance (a/b^2) than on parameters a and b, it is clear that the imputation method leads to an over-estimation of the sizes of the flaw indications. It consequently does not seem to be appropriate for the present study and it is not considered any more in the following. Note however that for all parameters, standard deviations are divided by two when the sample size is multiplied by four, which is an indicator of a "root–of–N" convergence rate with an asymptotic bias.

Table 2: Monte Carlo estimations for the NHP-HG model based on 500 simulated censored samples of size N (censoring level $c = 0.2$), without considering censoring (imputation method).

	N	a	b	a/b	a/b^2	α	β
value		1	2	0.5	0.25	1	1.5
	25	1.37	2.57	0.53	0.22	1.00	1.50
	50	1.37	2.58	0.53	0.21	1.00	1.50
mean	100	1.34	2.54	0.53	0.21	1.00	1.50
	228	1.31	2.49	0.52	0.21	1.00	1.50
	912	1.28	2.44	0.52	0.22	1.00	1.50
	25	0.39	0.62	0.03	0.05	0.12	0.05
	50	0.30	0.47	0.02	0.03	0.09	0.04
stand. err.	100	0.21	0.35	0.02	0.03	0.07	0.03
	228	0.14	0.23	0.01	0.02	0.05	0.02
	912	0.11	0.18	0.01	0.03	0.02	0.01
	25	[0.81, 2.13]	[1.67, 3.84]	[0.47, 0.58]	[0.15, 0.30]	[0.81, 1.18]	[1.43, 1.59]
	50	[0.94, 1.93]	[1.86, 3.45]	[0.49, 0.57]	[0.16, 0.27]	[0.86, 1.15]	[1.44, 1.57]
90% CI	100	[1.03, 1.70]	[2.03, 3.15]	[0.50, 0.55]	[0.17, 0.25]	[0.90, 1.11]	[1.46, 1.55]
	228	[1.09, 1.55]	[2.12, 2.89]	[0.50, 0.54]	[0.18, 0.24]	[0.93, 1.08]	[1.47, 1.53]
	912	[1.17, 1.40]	[2.28, 2.65]	[0.51, 0.53]	[0.20, 0.23]	[0.97, 1.04]	[1.48, 1.51]
	25	[0.76, 2.22]	[1.53, 3.91]	[0.47, 0.59]	[0.14, 0.33]	[0.78, 1.26]	[1.41, 1.60]
	50	[0.89, 2.07]	[1.81, 3.69]	[0.48, 0.58]	[0.15, 0.28]	[0.83, 1.17]	[1.43, 1.58]
95% CI	100	[0.99, 1.76]	[1.94, 3.27]	[0.49, 0.56]	[0.16, 0.26]	[0.87, 1.14]	[1.45, 1.56]
	228	[1.06, 1.60]	[2.08, 2.97]	[0.50, 0.55]	[0.18, 0.25]	[0.91, 1.09]	[1.46, 1.54]
	912	[1.15, 1.42]	[2.23, 2.67]	[0.51, 0.54]	[0.20, 0.23]	[0.96, 1.04]	[1.48, 1.52]

Estimation taking into account censoring. We first provide results in Table 3 for the same parameter sets as for the previous imputation method. The quality of the estimation

results is now good for both processes (NHP and HG). The previous bias on the HG process parameters almost disappears and, contrary to the results of Table 2, it decreases as the sample size increases. Confidence intervals are well centered on the true parameters values. Standard deviations are still divided by two as the sample size is multiplied by four, which means that the "root–of–N" convergence rate remains valid. Two other parameter sets are next considered in Tables 4 and 5 for $N \in \{25, 50, 100, 228\}$. The results mostly share the same good quality as for the first parameter set. The computation times are a little longer however: considering the estimation of one parameter set for $N = 228$ components, it takes about 70 central processing unit (c.p.u.) time for the first parameter set, 95 c.p.u. for the second one and 220 c.p.u. for the third one. This is due to the optimization step for the HG parameters which takes more time, apparently because of a flatter objective function to maximize.

Table 3: Monte Carlo estimations for the NHP-HG model based on 500 simulated censored samples of size N considering censoring (censoring level $c = 0.2$).

	N	a	b	a/b	a/b^2	α	β
value		1	2	0.5	0.25	1	1.5
mean	25	1.14	2.22	0.51	0.24	1.00	1.50
	50	1.08	2.13	0.51	0.24	1.00	1.50
	100	1.03	2.04	0.50	0.25	1.01	1.50
	228	1.03	2.04	0.50	0.25	1.00	1.50
	912	0.99	1.99	0.50	0.25	1.00	1.50
stand. err.	25	0.37	0.59	0.04	0.05	0.13	0.06
	50	0.23	0.38	0.02	0.04	0.09	0.04
	100	0.15	0.25	0.02	0.03	0.07	0.03
	228	0.12	0.20	0.01	0.04	0.04	0.02
	912	0.09	0.15	0.01	0.03	0.02	0.01
90% CI	25	[0.65, 1.87]	[1.44, 3.39]	[0.44, 0.57]	[0.16, 0.33]	[0.80, 1.22]	[1.41, 1.59]
	50	[0.76, 1.49]	[1.59, 2.83]	[0.47, 0.55]	[0.19, 0.30]	[0.87, 1.16]	[1.44, 1.57]
	100	[0.79, 1.29]	[1.66, 2.50]	[0.47, 0.53]	[0.21, 0.29]	[0.91, 1.11]	[1.45, 1.54]
	228	[0.88, 1.20]	[1.80, 2.33]	[0.48, 0.52]	[0.22, 0.28]	[0.93, 1.08]	[1.47, 1.53]
	912	[0.92, 1.07]	[1.86, 2.14]	[0.49, 0.51]	[0.24, 0.27]	[0.97, 1.04]	[1.48, 1.51]
95% CI	25	[0.57, 2.05]	[1.27, 3.61]	[0.43, 0.58]	[0.15, 0.37]	[0.76, 1.27]	[1.40, 1.61]
	50	[0.70, 1.61]	[1.52, 2.93]	[0.46, 0.55]	[0.18, 0.32]	[0.82, 1.19]	[1.43, 1.58]
	100	[0.76, 1.37]	[1.61, 2.64]	[0.47, 0.54]	[0.20, 0.30]	[0.88, 1.14]	[1.45, 1.55]
	228	[0.85, 1.25]	[1.75, 2.41]	[0.48, 0.52]	[0.22, 0.28]	[0.92, 1.09]	[1.47, 1.54]
	912	[0.90, 1.10]	[1.83, 2.17]	[0.49, 0.51]	[0.23, 0.27]	[0.96, 1.05]	[1.48, 1.52]

As a conclusion to this simulation study, it is clearly preferable to take censoring into consideration and doing so, the estimation procedure seems to provide reliable results (which can be more or less long to obtain according to the parameters).

4.2 Application to EDF data

EDF data concern $N = 228$ components. For confidentiality reasons the unit of the flaw indication measure is not specified. Each component has been inspected several times. The total

Table 4: Monte Carlo estimations for the NHP-HG model based on 500 simulated censored samples of size N considering censoring (censoring level $c = 6$).

	N	a	b	a/b	a/b^2	α	β
value		2	2	1	0.5	2	1
	25	2.35	2.31	1.01	0.48	2.01	1.00
mean	50	2.22	2.19	1.01	0.49	2.00	1.00
	100	2.13	2.11	1.00	0.49	2.01	1.00
	228	2.03	2.02	1.00	0.50	2.00	1.00
	25	0.86	0.75	0.06	0.14	0.24	0.05
stand. err.	50	0.66	0.58	0.05	0.14	0.18	0.04
	100	0.47	0.41	0.04	0.13	0.12	0.02
	228	0.29	0.25	0.03	0.09	0.08	0.02
	25	[1.13, 3.97]	[1.21, 3.67]	[0.90, 1.10]	[0.29, 0.76]	[1.62, 2.41]	[0.92, 1.08]
90% CI	50	[1.33, 3.55]	[1.42, 3.37]	[0.94, 1.07]	[0.31, 0.67]	[1.72, 2.29]	[0.95, 1.06]
	100	[1.48, 2.93]	[1.56, 2.83]	[0.95, 1.06]	[0.37, 0.62]	[1.83, 2.22]	[0.96, 1.04]
	228	[1.60, 2.51]	[1.65, 2.45]	[0.96, 1.04]	[0.42, 0.59]	[1.88, 2.12]	[0.97, 1.03]
	25	[1.05, 4.00]	[1.16, 3.75]	[0.88, 1.13]	[0.28, 0.80]	[1.56, 2.49]	[0.90, 1.11]
95% CI	50	[1.29, 3.79]	[1.34, 3.62]	[0.92, 1.09]	[0.29, 0.71]	[1.67, 2.33]	[0.94, 1.07]
	100	[1.40, 3.20]	[1.49, 2.97]	[0.94, 1.07]	[0.35, 0.64]	[1.79, 2.26]	[0.96, 1.05]
	228	[1.55, 2.64]	[1.60, 2.55]	[0.96, 1.04]	[0.40, 0.61]	[1.86, 2.14]	[0.97, 1.03]

Table 5: Monte Carlo estimations for the NHP-HG model based on 500 simulated censored samples of size N considering censoring (censoring level $c = 7.5$).

	N	a	b	a/b	a/b^2	α	β
value		2	1	2	2	3	0.75
	25	2.30	1.13	2.02	1.93	3.00	0.75
mean	50	2.15	1.07	2.01	1.95	3.01	0.75
	100	2.08	1.03	2.01	1.97	3.00	0.75
	228	2.03	1.01	2.00	2.01	3.01	0.75
	25	0.75	0.3	0.10	0.51	0.30	0.04
stand. err.	50	0.49	0.21	0.07	0.35	0.22	0.03
	100	0.35	0.15	0.05	0.25	0.16	0.02
	228	0.24	0.11	0.06	0.38	0.10	0.01
	25	[1.25, 3.89]	[0.66, 1.76]	[1.86, 2.20]	[1.21, 2.94]	[2.50, 3.55]	[0.69, 0.82]
90% CI	50	[1.43, 3.09]	[0.75, 1.46]	[1.89, 2.12]	[1.43, 2.60]	[2.63, 3.35]	[0.70, 0.80]
	100	[1.58, 2.69]	[0.82, 1.29]	[1.92, 2.10]	[1.60, 2.39]	[2.74, 3.26]	[0.71, 0.78]
	228	[1.70, 2.44]	[0.86, 1.19]	[1.95, 2.06]	[1.69, 2.28]	[2.83, 3.19]	[0.73, 0.77]
	25	[1.16, 3.96]	[0.62, 1.82]	[1.81, 2.23]	[1.17, 3.04]	[2.41, 3.61]	[0.68, 0.83]
95% CI	50	[1.32, 3.26]	[0.69, 1.55]	[1.86, 2.15]	[1.35, 2.74]	[2.59, 3.43]	[0.70, 0.81]
	100	[1.49, 2.82]	[0.77, 1.36]	[1.91, 2.11]	[1.53, 2.51]	[2.71, 3.30]	[0.71, 0.79]
	228	[1.63, 2.52]	[0.84, 1.23]	[1.94, 2.07]	[1.67, 2.33]	[2.80, 3.22]	[0.72, 0.78]

number of inspection times is 1,695. Our approach requires both numerical integration and numerical optimization for the computation and optimization of the log-composite-likelihood function provided by (11). To validate the estimation results, the `MATLAB` program used in the previous simulation study is used together with another one written in `R` [17]. The two programs provide very similar results. In addition, confidence intervals are computed via standard bootstrap method, using 1,000 sets of 228 trajectories uniformly drawn (with replacement) from the 228 trajectories of our data set. For each bootstrap sample, estimates are provided for the parameters. Empirical mean, standard deviation and both 90% and 95% confidence intervals are next derived for each parameter, based on the 1,000 estimation results. The 90% (resp. 95%) confidence interval corresponds to $[q_{0.05}, q_{0.95}]$ (resp. $[q_{0.025}, q_{0.975}]$), where q_α is the empirical $\alpha-$quantile based on the 1,000 estimation results. As often, this method is quite time consuming. Note that, based on the strong evidence provided by the previous Monte Carlo study for taking into account censoring, all the results of this section are computed under this basis.

Choosing between HP or NHP for the initiation process. Estimation results concerning the Poisson process (HP and NHP) are given in Table 6 (top) together with nonparametric bootstrap results. Note that whatever the model is, the estimates are within the bootstrapped confidence interval. For each model, Table 6 (bottom) next gives the yearly estimated average number of new indications. For the HP process, it is equal to $\hat{\lambda} \times 365$ whereas for the NHP process it is equal to $\hat{\alpha} \times \left\{(365\ k)^{\hat{\beta}} - (365\ \ (k-1))^{\hat{\beta}}\right\}$ for the k-th year (remember that the time unit is the day). In Table 6 (top), we can see that the 90% and 95% bootstrap confidences intervals for β do not contain the value 1, advocating for the selection of the NHP for the initiation process. Also, EDF experts consider that the rate of initiation of new indications should be increasing over time, leading here again to the choice of the NHP based on Table 6 (bottom).

Table 6: Estimation and bootstrap results based on 1,000 bootstrapped samples of size 228 for the parameters of the Poisson process (top: rows 3 to 7) and estimated yearly average number of new indications for one component (bottom: rows 8 to 12)

Model	HP	NHP			
Parameter	λ ($\times 10^{-4}$)	α ($\times 10^{-9}$)	β		
Estimation	1.56	1.22	2.28		
Mean	1.57	2.24	2.28		
St. dev.	0.17	2.60	0.13		
90% conf. int.	$[1.31, 1.85]$	$[0.18, 7.56]$	$[2.08, 2.49]$		
95% conf. int.	$[1.28, 1.91]$	$[0.12, 9.13]$	$[2.05, 2.54]$		
		Year 1	8.47×10^{-4}	Year 6	1.71×10^{-2}
Yearly average		Year 2	3.27×10^{-3}	Year 8	2.55×10^{-2}
number of new	5.71×10^{-2}	Year 3	6.26×10^{-3}	Year 10	3.45×10^{-2}
indications		Year 4	9.62×10^{-3}	Year 12	4.44×10^{-2}
		Year 5	1.33×10^{-2}	Year 15	5.92×10^{-2}

Choosing between HG and NHG for the propagation process. Estimation results are given in Table 7 (left) for the parameters of both HG and NHG degradation processes, considering both HP and NHP initiation processes. Table 7 (right) provides the annual mean

growth of one flaw indication considering the four models. As we can see, whatever the initiation process is (HP or NHP), in case of a NHG propagation process (with $A(t) = \eta t^{\gamma}$), the parameter γ is very small ($\gamma < 10^{-8}$) resulting in a strongly non-linear growth for one flaw indication, which essentially expands during the first year and next remains mostly constant. Based on EDF specialists considerations, we hence suggest to retain the homogeneous version of the gamma process (combined with an NHP process). However, this point might require further investigation. For example, a similar bootstrap method as for the initiation process model (HP vs. NHP) might be used, providing a bootstrap confidence interval for the unknown parameter γ. This would allow to test the null hypothesis $\gamma = 1$ (meaning that the gamma process is homogeneous). Unfortunately, we have faced the problem of huge calculation times and numerical instabilities. Thus, this approach could not be achieved.

Table 7: Estimation results for the propagation process on EDF data and the different models (left: columns 2 to 4), and the corresponding estimated expected annual growth for one flaw indication (right: columns 5 and 6)

Model	Estimates of the parameters of the gamma process			Expected annual growth of one flaw indication	
HP–HG		$\hat{a}$	$\hat{b}$	1.12	
		2.44×10^{-4}	0.08		
NHP–HG		$\hat{a}$	$\hat{b}$	1.97	
		8.63×10^{-4}	0.16		
HP–NHG	$\hat{\eta}$	$\hat{\gamma}$	$\hat{b}$	Year 1	11.61
	0.47	9.22×10^{-9}	0.04	Year 2	7.43×10^{-8}
NHP–NHG	$\hat{\eta}$	$\hat{\gamma}$	$\hat{b}$	Year 1	10.93
	0.36	2.24×10^{-10}	0.03	Year 2	1.70×10^{-9}

Estimation results for the selected NHP–HG model. Estimation results concerning the selected NHP–HG model are available in Table 8. The parameters are re–estimated using non-parametric bootstrap, which allows to obtain confidence intervals as well as standard deviations for the different parameters. Estimation results for the parameter b of the homogeneous gamma process are rather stable as well as for the parameter β of the initiation process. The results are less stable for the parameters α (initiation process) and a (homogeneous gamma process).

Table 8: Estimation (second line) and bootstrap (third line) results on EDF data based on $1,000$ bootstrapped samples of size 228 for the NHP–HG model parameters

	$\hat{\alpha}$ ($\times 10^{-9}$)	$\hat{\beta}$	$\hat{a}$ ($\times 10^{-4}$)	$\hat{b}$	$\hat{a}/\hat{b}$ ($\times 10^{-3}$)	$\hat{a}/\hat{b}^2$ ($\times 10^{-2}$)
Estimates	1.22	2.28	8.63	0.16	5.48	3.48
Mean	2.24	2.28	11.28	0.20	5.49	3.37
St. dev.	2.60	0.13	12.36	0.20	0.42	1.05
$[q_{0.05}, q_{0.95}]$	$[0.18, 7.56]$	$[2.08, 2.49]$	$[5.15, 19.55]$	$[0.10, 0.33]$	$[4.83, 6.20]$	$[1.73, 4.99]$
$[q_{0.025}, q_{0.975}]$	$[0.12, 9.13]$	$[2.05, 2.54]$	$[4.80, 26.72]$	$[0.10, 0.44]$	$[4.69, 6.31]$	$[1.35, 5.48]$

Additional prognostic indicator evaluation. All the computations of this paragraph have been carried out with `MATLAB`. The estimation results concerning the initiation time of the first flaw indication are given in Table 9. As we saw in Section 2.3, the initiation time is Weibull distributed. The estimated mean is close to 19 years with a standard deviation estimated to 9 years. From the bootstrap study, the results seem to be reliable.

Table 9: Mean and standard deviation (St. dev.) of the initiation time of the first flaw indication on the EDF data and inference results based on 10^3 bootstrapped samples of size 228

	Mean (years)		Standard deviation (years)	
Estimation	19.61		9.11	
	Mean [St. dev.]	$[q_{0.025}, q_{0.975}]$	Mean [St. dev.]	$[q_{0.025}, q_{0.975}]$
Bootstrap	19.65 [0.83]	[18.16, 21.40]	9.18 [0.64]	[8.05,10.53]

The yearly propagation of one flaw indication is next provided in Table 10, which is about 2 units in average, as confirmed by the bootstrap results. Note that the yearly propagation of one flaw indication based on the process $(Z_t)_{t\geq 0}$ is necessarily larger since it corresponds to the largest indication.

Table 10: Yearly mean growth of one flaw indication for EDF data using the NHP–HG model and associated bootstrap results based on $1,000$ samples of size 228

Estimation	2.00		
	Mean [St. dev.]	$[q_{0.05},q_{0.95}]$	$[q_{0.025},q_{0.975}]$
Bootstrap	2.01 [0.15]	[1.76,2.26]	[1.71,2.30]

We finish this section with estimation results for the quantile of the residual life $\tau_{90} - t_0$ given $(Z_{t_0}, N_{t_0}) = (z_0, n_0)$ for the critical level $\ell = 90$. First, Figure 2 depicts the estimated quantile curve $\varepsilon \mapsto \hat{t}_\varepsilon^{(90,t_0,z_0,n_0)}$ of the residual life as a function of ε (the time scale is given in years) for three different values of (ℓ, t_0, z_0, n_0). We can see that, for each value of (t_0, z_0, n_0), the ε–quantile increases with ε. Looking at the boundary values for ε (0^+ and 1^-), we can also see that the ε–quantile quickly increases (towards ∞) when ε approaches to 1^- and quickly decreases (towards 0) when ε goes to 0^+. These observations are consistent with what might have been expected. Second, we consider components for which no flaw indication has appeared at the end of the observation period (denoted by t_0), that is components for which $z_0 = 0$, and thus $n_0 = 0$, at time $t_0 > 0$. Corresponding quantiles $t_\varepsilon^{(90,0,0)}$ are given for several values of ε ($\varepsilon \in \{0.9, 0.95\}$) in Table 11. The mean and standard deviation values are calculated using the non-parametric bootstrap method. Figure 3 plots similar quantiles with respect to t_0 for ε equal to 0.75, 0.9 and 0.95. Table 12 finally provides estimated ε–quantiles of the residual life $\tau_{90} - t_0$ given various values of (z_0, n_0) at time $t_0 = 25$ and $\varepsilon \in \{0.75, 0.9, 0.95\}$. Looking at Figure 3 and Table 12, we can see that, as expected and for a given ε, the ε–quantile is decreasing with respect of t_0, z_0 and n_0. Also, we can conclude from these results that the residual life of a component is clearly influenced by the observed number of initiated flaw indications, which consequently should continue to be collected.

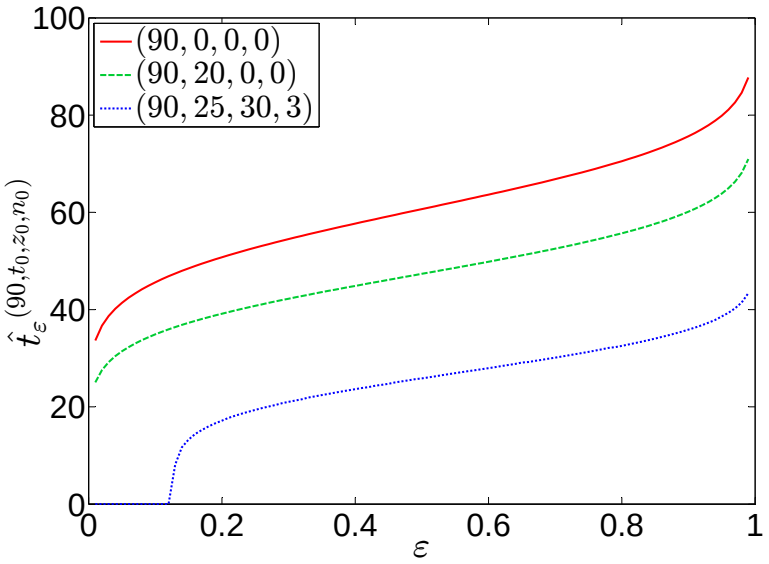

Figure 2: Estimated ε–quantile $\hat{t}_\varepsilon^{(90,t_0,z_0,n_0)}$ of the residual life $\tau_{90} - t_0$ (in years) with respect of $\varepsilon \in (0,1)$ for three different values of (t_0, z_0, n_0)

Table 11: Estimation of $t_\varepsilon^{(90,0,0)}$, the quantiles of order ε of the hitting time of level $\ell = 90$ for $z_0 = 0$ at $t_0 = 0$ and inference results based on 10^3 bootstrapped samples of size 228

ε	0.9		0.95	
Data	75.65		79.87	
	Mean [St. dev.]	$[q_{0.05}, q_{0.95}]$	Mean [St. dev.]	$[q_{0.05}, q_{0.95}]$
Bootstrap	75.89 [4.57]	[69.66, 83.66]	80.09 [5.25]	[73.41, 88.58]

Table 12: Estimated ε–quantiles of the residual life $\tau_{90} - t_0$ given various values of (z_0, n_0) at time $t_0 = 25$ and $\varepsilon \in \{0.75, 0.9, 0.95\}$

t_0	z_0	n_0	$t_{0.75}^{(\ell,t_0,z_0,n_0)}$	$t_{0.90}^{(\ell,t_0,z_0,n_0)}$	$t_{0.95}^{(\ell,t_0,z_0,n_0)}$	t_0	z_0	n_0	$t_{0.75}^{(\ell,t_0,z_0,n_0)}$	$t_{0.90}^{(\ell,t_0,z_0,n_0)}$	$t_{0.95}^{(\ell,t_0,z_0,n_0)}$
25	20	2	36.681	41.480	44.283	25	40	2	29.611	34.494	37.473
25	20	4	32.264	36.660	39.225	25	40	4	26.562	30.974	33.580
25	20	6	29.381	33.580	35.981	25	40	6	24.380	28.716	31.008
25	20	8	27.052	31.402	33.652	25	40	8	22.631	26.859	29.214
25	20	10	25.119	29.683	31.904	25	40	10	21.046	25.395	27.647
25	30	2	33.404	38.362	41.142	25	50	2	25.141	29.981	32.880
25	30	4	29.622	34.023	36.558	25	50	4	22.954	27.470	30.054
25	30	6	27.070	31.311	33.637	25	50	6	21.252	25.560	28.051
25	30	8	25.093	29.258	31.571	25	50	8	19.749	24.076	26.345
25	30	10	23.341	27.655	29.876	25	50	10	18.374	22.781	25.125

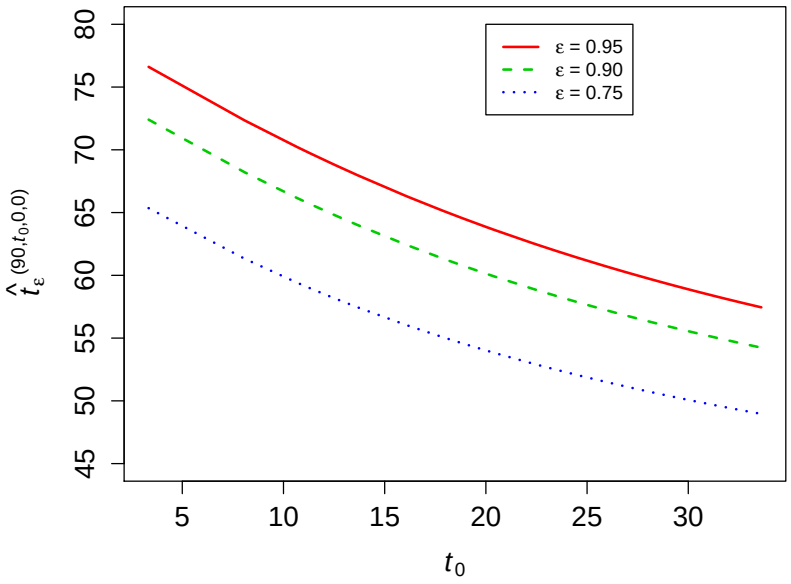

Figure 3: Estimated ε–quantiles of the residual life $\tau_{90} - t_0$ (in years) given $z_0 = n_0 = 0$ at time $t_0 > 0$ with respect of t_0 for $\varepsilon \in \{0.75, 0.9, 0.95\}$

5 Concluding remarks

We proposed a stochastic model for the competing degradation process $(N_t, Z_t)_{t\geq 0}$ describing initiation and propagation of degradation on a passive component of an electric power plant. This model associates a Poisson process together with a gamma process, where both processes may be homogeneous or not. This leads to four different models, which have been fitted to EDF data. The final retained model is based on a bootstrap confidence interval for the shape parameter of the non homogeneous Poisson process and on EDF experts considerations for the gamma process. It is a combination of a NHP process for the initiation of the flaw indications and a HG process for describing the growth of the indications.

The Monte Carlo simulation study shows that the sample size of the EDF data is sufficient to guarantee the quality of estimation results. The study also shows that taking into account censoring is necessary to avoid some bias on the estimates of the gamma process parameters. This bias disappears when accounting for censoring.

The 95% confidence intervals obtained on the EDF data may appear as rather large for some parameters such as a or α. However, looking at the confidence intervals for the indicators of interest (mean and standard deviation of the initiation time of the first flaw indication, yearly mean growth of one flaw indication, ε–quantiles of the residual life) provided in Tables 9, 10 and 11, we can see that they are not so large. The estimated indicators hence appear as accurate enough for helping the decision process (e.g. deciding whether the component should be replaced or not). The influence of the number of initiated flaw indications on a component residual life is also made clear by the study. It is hence of a major importance to go on collecting these data from the field, and to take this degradation indicator into account for prognostic purpose.

From a statistical point of view, studying the asymptotic behavior of our parametric esti-

mators and selecting one model are challenging objectives. The later point requires to use some information criteria like AIC (see [24]) or BIC (see [9]), previously developed in the composite likelihood approach as defined by Lindsay [15]. The use of these criteria would require the preliminary adaptation of our estimation method, which is based on a two-step procedure plus a composite likelihood method (see [9] for some recent results concerning BIC selection model criteria for composite likelihood approach).

Another challenging statistical issue would be to integrate measurement errors in our model, with two possible levels of errors. The first level deals with the number of initiated flaw indications, where typically, too small indications may be unrevealed by the testing processes. The second level is linked to the sizing process, which may be perturbed by measurement errors.

Finally, the possibility to include a time influence on the degradation dynamic could be considered by including a time effect on the degradation rate. For instance one could consider a similar model where the i–th degradation process has a shape parameter depending on its initiation time T_i: $a = \exp(\theta T_i)$ where $\theta \in (0, +\infty)$. Note however that this model requires further investigation since the T_i's are generally interval censored.

Acknowledgements The authors thank the Associate Editor and the two Referees for their very careful reading of the paper and for their deep questions, which have helped us to highly improve the paper.

This work was supported by the French National Research Agency (ANR), AMMSI project, ref. ANR-2011-BS01-021.

References

[1] Abdel-Hammed, M. (1975). A gamma wear process. *IEEE Transactions on Reliability*, 24(2), 152–153.

[2] Balakrishnan, N. and Pal, S. (2014). COM-Poisson Cure Rate Models and Associated Likelihood-based Inference with Exponential and Weibull Lifetimes. *Applied Reliability Engineering and Risk Analysis*, 308–348, John Wiley & Sons, Ltd.

[3] Caballé, N. C., Castro, I. T., Pérez, C. J. and Lanza-Gutiérrez, J. M. (2015). A condition-based maintenance of a dependent degradation-threshold-shock model in a system with multiple degradation processes. *Reliability Engineering and System Safety*, 134, 98–109.

[4] Castro, I. T. , Barros, A. and Grall, A. (2011). Age-based preventive maintenance for passive components submitted to stress corrosion cracking. *Mathematical and Computer Modelling*, 54(1-2), 598–609.

[5] Castro, I. T. , Caballé, N. C. and Pérez, C. J. (2015). A condition-based maintenance for a system subject to multiple degradation processes and external shocks. *International Journal of Systems Science*, 46(9), 1692–1704.

[6] Cha, J. H. and Castro, I. T. (2015). A stochastic failure model with dependent competing risks and its applications to condition-based maintenance. *Journal of Applied Probability*, 52(2), 558–573.

[7] Cox, D. and Reid, N. (2004). A note on pseudolikelihood constructed from marginal densities. *Biometrika*, 91, 729–737.

[8] Crowder, M. (2001). *Classical Competing Risks*, Chapman & Hall/CRC.

[9] Gao, X. and Song, P. X. K. (2010). Composite likelihood bayesian information criteria for model selection in high-dimensional data. *Journal of the American Statistical Association*, 105(492), 1531–1540.

[10] Guida, M. and Penta, F. (2015). A gamma process model for the analysis of fatigue crack growth data. *Engineering Fracture Mechanics*, 142, 21–49.

[11] Haghighi, F. and Nazeri Rad, N. (2011). Parametric degradation model with multiple competing risks. *Quality Technology and Quantitative Management*, 8(4), 389–400.

[12] Kahle, W., Mercier, S. and Paroissin, C. (2016). *Degradation Processes in Reliability*. ISTE Ltd and John Wiley & Sons, Inc. Under press.

[13] Kuniewski, S. P., van der Weide, J. A. M. and van Noortwijk, J. M. (2009). Sampling inspection for the evaluation of time-dependent reliability of deteriorating systems under imperfect defect detection. *Reliability Engineering and System Safety*, 94, 1480–1490.

[14] Lemaire, M. (2013). *Structural Reliability*, John Wiley & Sons.

[15] Lindsay, B. (1988). "Composite likelihood methods" in *Statistical Inference from Stochastic Processes*, ed. N. U. Prabhu, Providence, RI: American Mathematical Society, pp. 221–239.

[16] MATLAB (2010). Version 7.10.0 (R2010a). Natick, Massachusetts: The MathWorks Inc.

[17] R Development Core Team (2015). R: A language and environment for statistical computing. R Foundation for Statistical Computing, Vienna, Austria.

[18] Ross, S. N. (1996). *Stochastic processes.* Wiley, New York.

[19] Scarf, P. A., Wang, W. and Laycock P. J. (1996). A stochastic model of crack growth under periodic inspections. *Reliability Engineering & System Safety*, 51(3), 331–339.

[20] Singpurwalla, N. (2006). On competing risk and degradation processes. *IMS Lecture Notes-Monograph Series, 2nd LehmannSymposium – Optimality*, 49, 229–240.

[21] Somboonsavatdee, A. and Sen, A. (2015). Parametric inference for multiple repairable systems under dependent competing risks. *Applied Stochastic Models in Business and Industry*, 31(5), 706–720.

[22] van Noortwijk, J. M. (2009). A survey of the application of gamma processes in maintenance. *Reliability Engineering and System Safety*, 94, 2–21.

[23] Varin, C., Reid, N. and Firth, D. (2011). An overview of composite likelihood methods. *Statistica Sinica*, 21, 5–42.

[24] Varin, C. and Vidoni, P. (2005). A note on composite likelihood inference and model selection. *Biometrika*, 92(3), 519–528.

[25] Velázquez, J. C., Van Der Weide, J. A. M., Hernández, Enrique and Hernández, Héctor Herrera (2014). Statistical modelling of pitting corrosion: Extrapolation of the maximum pit depth-growth. *International Journal of Electrochemical Science*, 9, 4129–4143.

[26] Ye, Z.-S. and Xie, M. (2015). Stochastic modelling and analysis of degradation for highly reliable products. *Applied Stochastic Models in Business and Industry*, 31(1), 16–32.

Appendix A Conditional distribution of Z_t given $N_t = n$

The case $n = 0$ is clear so that only the case $n \geq 1$ is considered.
For $n \geq 1$ and $z \geq 0$, we have

$$\begin{aligned}\mathbb{P}\left(Z_t \leq z | N_t = n\right) &= \mathbb{P}\left(\max_{0\leq i\leq n} X^{(i)}_{t-T_i} \leq z | N_t = n\right) \\ &= \mathbb{P}\left(\bigcap_{i=1}^{n}\left\{X^{(i)}_{t-T_i} \leq z\right\} | N_t = n\right).\end{aligned}$$

Given that $N_t = n$, the random vector $(T_1, \ldots, T_n)$ is known to be identically distributed as the order statistics $\left(Y^{(1)}, \ldots, Y^{(n)}\right)$ obtained from n i.i.d. copies Y_1, ..., Y_n of a random variable Y with p.d.f.

$$f_Y\left(y\right) = \frac{\lambda\left(y\right)}{\Lambda\left(t\right)}\mathbf{1}_{[0,t]}\left(y\right), \tag{A.1}$$

see for instance [18, Problem 2.32 p. 95].
Based on the independence between the $X^{(i)}$'s and N_t, we obtain

$$\mathbb{P}\left(Z_t \leq z | N_t = n\right) = \mathbb{P}\left(\bigcap_{i=1}^{n}\left\{X^{(i)}_{t-Y^{(i)}} \leq z\right\}\right) = \mathbb{P}\left(\bigcap_{i=1}^{n}\left\{X^{(i)}_{t-Y_i} \leq z\right\}\right),$$

using that the probability of $\bigcap_{i=1}^{n}\left\{X^{(i)}_{t-Y^{(i)}} \leq z\right\}$ does not depend on the order of the $Y^{(i)}$'s for the last equality. Conditioning by the Y_i's and remembering that $F_{A(u),b}$ is the common c.d.f. of the $X^{(i)}_u$'s (and using the independence between the $X^{(i)}$'s and the Y_i's), we now have

$$\begin{aligned}\mathbb{P}\left(Z_t \leq z | N_t = n\right) &= \mathbb{E}\left(\prod_{k=1}^{n} F_{A(t-Y_i),b}\left(z\right)\right) \\ &= \left\{\mathbb{E}\left[F_{A(t-Y),b}\left(z\right)\right]\right\}^n \\ &= \left\{\frac{\int_0^t F_{A(y),b}\left(z\right)\lambda\left(t-y\right)dy}{\Lambda\left(t\right)}\right\}^n\end{aligned}$$

based on the i.i.d. property of the Y_i's for the second line and on the fact that the common p.d.f. of the Y_i's is provided by (A.1) for the last line.
The derivation of the p.d.f. with respect to Lebesgue measure of the conditional distribution of Z_t given $N_t = n$ is now clear, which achieves this proof.

Appendix B Proof of Proposition 2

First we consider the case $z_0 = 0$ (or equivalently: $n_0 = 0$). Let us first observe that given $N_{t_0} = 0$, the random variable N_t is conditionally Poisson distributed with parameter

$$\begin{aligned}\tilde{\Lambda}(t) &= \left(\Lambda(t) - \Lambda(t_0)\right)^+ = \int_{t_0}^{t} \tilde{\lambda}(u)\, du, \\ \tilde{\lambda}(t) &= \lambda(t)\mathbf{1}_{[t_0,\infty)}(t)\end{aligned}$$

whatever $t < t_0$ or $t \geq t_0$. Now, let us set $\tilde{\mathbb{P}}(\cdot) = \mathbb{P}(\cdot|N_{t_0} = 0)$. Under $\tilde{\mathbb{P}}$, it is easy to check that the counting process $(N_t)_{t\geq 0}$ still has independent increments. Based on the previous remark, $(N_t)_{t\geq 0}$ hence is a Poisson process under $\tilde{\mathbb{P}}$, with rate function $\tilde{\lambda}(\cdot)$. For $t \geq t_0$ and $n \geq 0$, we consequently have

$$\begin{aligned}\mathbb{P}(Z_t \leq z|N_{t_0} = 0, N_t = n) &= \tilde{\mathbb{P}}(Z_t \leq z|N_t = n)\\ &= \left\{\frac{\int_0^t F_{A(y),b}(z)\tilde{\lambda}(t-y)dy}{\tilde{\Lambda}(t)}\right\}^n\end{aligned}$$

where the second equality holds by Proposition 1. Then we derive

$$\begin{aligned}\mathbb{P}(Z_t \leq z|Z_{t_0} = 0) &= \sum_{n\geq 0}\mathbb{P}(Z_t \leq z|N_{t_0} = 0, N_t = n)\mathbb{P}(N_t = n)\\ &= \sum_{n\geq 0}\left\{\frac{\int_0^t F_{A(y),b}(z)\tilde{\lambda}(t-y)dy}{\tilde{\Lambda}(t)}\right\}^n e^{-\tilde{\Lambda}(t)}\frac{\tilde{\Lambda}(t)^n}{n!}\\ &= e^{-(\Lambda(t)-\Lambda(t_0))+\int_0^{t-t_0}F_{A(y),b}(z)\lambda(t-y)dy}\\ &= e^{-\int_{t_0}^t \bar{F}_{A(t-v),b}(z)\lambda(v)dv}.\end{aligned}$$

Second we consider the case $z_0 > 0$ (or equivalently: $n_0 > 0$). Let (t, n, z) such that $t_0 < t$, $n_0 \leq n$ and $z_0 \leq z$. We have:

$$\begin{aligned}&\mathbb{P}\left(Z_{t_0} \leq z_0, N_{t_0} = n_0, Z_t \leq z, N_t = n\right)\\ &= \mathbb{P}\left(\bigcap_{i=1}^{n_0}\left\{X^{(i)}_{t_0-T_i} \leq z_0\right\} \cap \bigcap_{i=1}^{n}\left\{X^{(i)}_{t-T_i} \leq z\right\} \cap \{N_{t_0} = n_0\} \cap \{N_t = n\}\right)\\ &= \mathbb{P}\left(\bigcap_{i=1}^{n_0}\left\{X^{(i)}_{t_0-T_i} \leq z_0, X^{(i)}_{t-T_i} \leq z\right\} \cap \bigcap_{i=n_0+1}^{n}\left\{X^{(i)}_{t-T_i} \leq z\right\} \cap \{N_{t_0} = n_0\} \cap \{N_t = n\}\right)\end{aligned}$$

(using the convention that if $n_0 = n$, the corresponding empty intersection is equal to Ω). Conditioning by $\sigma\left((N)_{t\geq 0}, \left\{X^{(i)} \text{ for } 1 \leq i \leq n_0\right\}\right)$, we get

$$\begin{aligned}&\mathbb{P}\left(Z_{t_0} \leq z_0, N_{t_0} = n_0, Z_t \leq z, N_t = n\right)\\ &= \mathbb{E}\left(\prod_{i=1}^{n_0}\mathbf{1}_{\left\{X^{(i)}_{t_0-T_i} \leq z_0, X^{(i)}_{t-T_i} \leq z\right\}}\prod_{i=n_0+1}^{n}F_{A(t-T_i),b}\left(z\right)\mathbf{1}_{\left\{N_{t_0}=n_0\right\}}\mathbf{1}_{\{N_t=n\}}\right).\end{aligned}$$

Writing $X^{(i)}_{t-T_i} = X^{(i)}_{t_0-T_i} + \left(X^{(i)}_{t-T_i} - X^{(i)}_{t_0-T_i}\right)$ and using the independent increments of $X^{(i)}$, we obtain through conditioning by $\sigma\left((N)_{t\geq 0}, \left\{X^{(i)}_{t_0-T_i} \text{ for } 1 \leq i \leq n_0\right\}\right)$

$$\begin{aligned}&\mathbb{P}\left(Z_{t_0} \leq z_0, N_{t_0} = n_0, Z_t \leq z, N_t = n\right)\\ &= \mathbb{E}\left(\prod_{i=1}^{n_0}\mathbf{1}_{\left\{X^{(i)}_{t_0-T_i} \leq z_0\right\}}F_{A(t-T_i)-A(t_0-T_i),b}\left(z - X^{(i)}_{t_0-T_i}\right)\prod_{i=n_0+1}^{n}F_{A(t-T_i),b}\left(z\right)\mathbf{1}_{\left\{N_{t_0}=n_0\right\}}\mathbf{1}_{\{N_t=n\}}\right)\\ &= \mathbb{E}\left(\prod_{i=1}^{n_0}\varphi_1\left(T_i\right)\prod_{i=n_0+1}^{n}\varphi_2\left(T_i\right)\mathbf{1}_{\left\{N_{t_0}=n_0\right\}}\mathbf{1}_{\{N_t=n\}}\right)\end{aligned}$$

where

$$\begin{aligned}\varphi_1(u) &= \mathbb{E}\left\{\mathbf{1}_{\left\{X^{(i)}_{t_0-u}\leq z_0\right\}} F_{A(t-u)-A(t_0-u),b}\left(z - X^{(i)}_{t_0-u}\right)\right\}\\ &= \int_0^{z_0} F_{A(t-u)-A(t_0-u),b}(z-x)\, f_{A(t_0-u),b}(x)\, dx,\\ \varphi_2(u) &= F_{A(t-u),b}(z).\end{aligned}$$

Given that $\{N_{t_0} = n_0, N_t = n\}$, the random vector $(T_1, \ldots, T_{n_0})$ is conditionally identically distributed as the order statistic $\left(Y^{(1)}, \ldots, Y^{(n_0)}\right)$ of the same i.i.d. Y_i's as in (A.1) whereas the random vector $(T_{n_0+1}, \ldots, T_n)$ can be seen to be conditionally identically distributed as the order statistic $(V^{(n_0+1)}, \ldots, V^{(n)})$, where $V_{n_0+1}, \ldots, V_n$ are i.i.d. copies of a random variable V with p.d.f. provided by

$$f_V(v) = \frac{\lambda(v)}{\Lambda(t) - \Lambda(t_0)} \mathbf{1}_{[t_0,t]}(v). \tag{B.1}$$

Also, the vectors $(T_1, \ldots, T_{n_0})$ and $(T_{n_0+1}, \ldots, T_n)$ are conditionally independent. This provides

$$\begin{aligned}&\mathbb{P}(Z_{t_0} \leq z_0, Z_t \leq z | N_{t_0} = n_0, N_t = n)\\ &= \mathbb{E}\left(\prod_{i=1}^{n_0} \varphi_1(Y_i) \prod_{i=n_0+1}^{n} \varphi_2(V_i)\right)\\ &= \left(\mathbb{E}(\varphi_1(Y))\right)^{n_0} \left(\mathbb{E}(\varphi_2(V))\right)^{n-n_0}\\ &= \left\{\int_0^{t_0} \varphi_1(y) \frac{\lambda(y)}{\Lambda(t_0)} dy\right\}^{n_0} \times \left\{\int_{t_0}^{t} \varphi_2(v) \frac{\lambda(v)}{\Lambda(t) - \Lambda(t_0)} dv\right\}^{n-n_0}\end{aligned}$$

and based on the independent increments of the Poisson process $(N_t)_{t\geq 0}$, we get

$$\begin{aligned}&\mathbb{P}(Z_{t_0} \leq z_0, N_{t_0} = n_0, Z_t \leq z, N_t = n)\\ &= \mathbb{P}(Z_{t_0} \leq z_0, Z_t \leq z | N_{t_0} = n_0, N_t = n)\, \mathbb{P}(N_{t_0} = n_0)\, \mathbb{P}(N_t - N_{t_0} = n - n_0)\\ &= \left\{\int_0^{t_0} \varphi_1(y)\, \lambda(y)\, dy\right\}^{n_0} \times \left\{\int_{t_0}^{t} \varphi_2(v)\, \lambda(v)\, dv\right\}^{n-n_0} \frac{e^{-\Lambda(t)}}{n_0!\,(n-n_0)!}\end{aligned}$$

after simplification.

Substituting φ_1 and φ_2 by their expressions, we now have

$$\begin{aligned}&\mathbb{P}(Z_{t_0} \leq z_0, N_{t_0} = n_0, Z_t \leq z, N_t = n)\\ &= \left\{\int_0^{t_0} \left(\int_0^{z_0} F_{A(t-u)-A(t_0-u),b}(z-x)\, f_{A(t_0-u),b}(x)\, dx\right) \lambda(u)\, du\right\}^{n_0}\\ &\times \left\{\int_{t_0}^{t} F_{A(t-v),b}(z)\, \lambda(v)\, dv\right\}^{n-n_0} \frac{e^{-\Lambda(t)}}{n_0!\,(n-n_0)!}\end{aligned}$$

and

$$\begin{aligned}
&\mathbb{P}\left(Z_{t_0} \in dz_0, N_{t_0} = n_0, Z_t \leq z, N_t = n\right) \\
&= \int_0^{t_0} F_{A(t-u)-A(t_0-u),b}\left(z - z_0\right) f_{A(t_0-u),b}\left(z_0\right) \lambda\left(u\right) du \\
&\times \left\{ \int_0^{t_0} \left(\int_0^{z_0} F_{A(t-u)-A(t_0-u),b}\left(z - x\right) f_{A(t_0-u),b}\left(x\right) dx \right) \lambda\left(u\right) du \right\}^{n_0-1} \\
&\times \left\{ \int_{t_0}^{t} F_{A(t-v),b}\left(z\right) \lambda\left(v\right) dv \right\}^{n-n_0} \frac{e^{-\Lambda(t)}}{(n_0-1)!\,(n-n_0)!}\, dz_0. \qquad \text{(B.2)}
\end{aligned}$$

Using Appendix A or (B.2), one easily gets

$$\begin{aligned}
&\mathbb{P}\left(Z_{t_0} \in dz_0, N_{t_0} = n_0\right) \\
&= \frac{e^{-\Lambda(t_0)}}{(n_0-1)!} \left(\int_0^{t_0} F_{A(t_0-y),b}\left(z_0\right) \lambda\left(y\right) dy \right)^{n_0-1} \times \left(\int_0^{t_0} f_{A(t_0-y),b}\left(z_0\right) \lambda\left(y\right) dy \right) dz_0 \qquad \text{(B.3)}
\end{aligned}$$

from where we finally derive Equation (5) by dividing (B.2) by (B.3).

Appendix C Proof of Proposition 3

First case: $\mathbf{z_0 = 0}$. Based on Equation (4), the quantile $t_\varepsilon^{(\ell,t_0,0)}$ verifies

$$-\int_{t_0}^{t_0+t_\varepsilon^{(\ell,t_0,0)}} \bar{F}_{a\left(t_\varepsilon^{(\ell,t_0,0)}+t_0-v\right),b}\left(\ell\right) \lambda\left(v\right) dv = \log\left(1-\varepsilon\right)$$

which may easily be written as (6).

Second case: $\mathbf{z_0 > 0}$. We write $t_\varepsilon = t_\varepsilon^{(\ell,t_0,z_0,n_0)}$ for sake of simplicity. Based on Corollary 1 and in case of a homogeneous gamma process, the quantile t_ε is the solution of

$$\begin{aligned}
&\log\left\{F_{a\,t_\varepsilon,b}\left(\ell - z_0\right)\right\} - \int_0^{t_\varepsilon} \lambda\left(t_0+u\right) \bar{F}_{a(t_\varepsilon-u),b}\left(\ell\right) du \\
&+ \left(n_0-1\right) \log\left\{ \int_0^{t_0} \lambda\left(u\right) \left(\int_0^{z_0} F_{a\,t_\varepsilon,b}\left(\ell - x\right) f_{a(t_0-u),b}\left(x\right) dx \right) du \right\} \\
&- \left(n_0-1\right) \log\left\{ \int_0^{t_0} F_{a(t_0-y),b}\left(z_0\right) \lambda\left(y\right) dy \right\} \\
&= \log\left(1-\varepsilon\right),
\end{aligned}$$

which may easily be written as (7).